Effects of periodicity perturbations on the transmission by underwater phononic crystals

K. Zong, H. Franklin,[a] and O. Lenoir
Laboratoire Ondes et Milieux Complexes UMR CNRS 6294, Université du Havre, Place R. Schuman BP 4006, 76610 Le Havre, France

M. V. Predoi
Department of Mechanics, University Politehnica Bucharest, Splaiul Independentei 313, Bucharest, Romania

The effects of periodicity perturbations in underwater phononic crystal layers composed of noninterpenetrating rows of identical shells are investigated. The results for one row are obtained by using a multiple scattering method between shells. Then, taking into account the multiple reflections and transmissions between two adjacent rows, a Debye series method is used to calculate the reflection and transmission coefficients by a finite number of rows. The paper focuses on three kinds of perturbations: (i) variation of the inner radius of shells from row to row, (ii) increase in the spacing from row to row and of the number of rows, and (iii) substitution of simple steel rows by steel-polyethylene bilayers. It is shown by studying the transmission coefficient that the case (i) permits the insertion of narrow pass bands in the stop band while the two other cases (ii) and (iii) widen the stop band. The study intends to model simple underwater acoustic filters.
© 2012 Acoustical Society of America. [http://dx.doi.org/10.1121/1.4744976]

I. INTRODUCTION

The existence of band gaps in phononic crystals (one-dimensional or two-dimensional vibrating periodic structures) suggests various applications such as design of underwater ultrasonic silent materials by using compliant tubes,[1] nondestructive testing of immersed tube bundles and surveillance techniques,[2,3] design of acoustic waveguides with selective frequencies or filters by considering square arrays of steel cylinders in water containing defects created by substitution of one row or more by hollow cylinders.[4] The reflectance properties of sonic band gap materials made up of rigid cylinders in air,[5] the engineering of large acoustic band gaps by considering rigid or liquid cylinders in a liquid,[6] or large elastic band gaps by means of periodic air inclusions and aluminum cylinders in an epoxy matrix[7] are also thoroughly studied. It should be noted that the cylinders are assumed infinitely long in cited references.

In the present work, we investigate the influence of several types of perturbations in phononic crystal layers composed in all cases of identical steel shells placed on rows. These perturbations include variations of the inner radius of shells from a row to its neighbor, the spacing between rows, the spacing between shells in a given row, and the substitution of steel rows by steel-polyethylene bilayers. The effect of the number of gratings is also investigated.

Among the methods frequently applied to the calculations of band structures of phononic crystals and of reflection and transmission coefficients of finite systems of phononic crystals (slabs), we have chosen the multiple scattering method developed for cylindrical[8–10] and spherical scatterers,[11] exactly as presented in Refs. 1–3 and 12, for instance. The same method has been used for fluid cavities in an elastic matrix.[13] The first part of the method is devoted to a multiple scattering calculation between the scatterers forming one row and then allows us to find the scattering properties of this row, e.g., the reflection and transmission coefficients. The second part considers that the slab is made up of a sequence of periodically or not arranged rows, each one with known reflection and transmission coefficients. Between two consecutive rows denoted as *A* and *B*, multiple reflections and transmissions take place and the waves superimpose. For an incident wave propagating from *A* to *B*, the reflection coefficient directly from the row A and the transmission through the row *B* are obtained in terms of geometric series. A sequence of more than two rows can be treated iteratively in the same way to obtain the reflection and transmission coefficients by the slab. The multiple scattering method is numerically efficient and allows easy variation in both geometrical and physical parameters in the phononic crystal.

In Sec. II, we recall the resonant properties of a single shell. Two types of resonance families are highlighted, either those related to circumferential waves propagating in the thickness of a shell, or those related to the waves propagating in the inner water column. In Sec. III, the expressions of the reflection and transmission coefficients by single rows of identical and regularly spaced shells are given. They are obtained by using the multiple scattering method. Numerical results are provided. In Sec. IV, we first present results (Sec. IV A) dealing with lattices composed of a finite number of rows of identical shells with identical spacings between shells and between rows. They are used as a reference. In Sec. IV B, variations of the inner radius of shells from row to

---

[a]Author to whom correspondence should be addressed. Electronic mail: herve.franklin@univ-lehavre.fr

row are dealt with. In Sec. IV C, the influence of an increase in the spacing between rows from the insonified face is investigated. The influence of the number of rows is also analyzed. In Sec. IV D, the steel rows are replaced by steel-polyethylene bilayers. In each case, the transmission coefficient is studied and compared to the one of reference. We focus particularly on the effects of periodicity perturbations on the stop bands.

II. SCATTERING BY AN ELASTIC SHELL AT NORMAL INCIDENCE

Consider a plane pressure wave $p_{inc} = e^{i(kx-\omega t)}$, normally incident on an infinitely long cylindrical steel shell of axis z immersed in water of density $\rho = 1000 \, \text{kg/m}^3$ and sound velocity $c = 1470 \, \text{m/s}$. Here, ω denotes the angular frequency, t is the time, and $k = \omega/c$ is the wavenumber in the fluid. For steel, the density is $\rho_s = 7900 \, \text{kg/m}^3$, the longitudinal and transverse velocities are $c_l = 5790 \, \text{m/s}$ and $c_t = 3100 \, \text{m/s}$. The relative thickness of the shell is fixed by the ratio b/a where a and b denote the outer and the inner radius of the shell, respectively. At a fixed point $P(r,\theta)$ of the plane (Ox,Oy) and in the outer fluid [r denotes the distance from the center O of the shell to the observation point P and θ is the angle (Ox,OP)], the acoustic pressure scattered by the shell has the form[14,15]

$$p_s = e^{-i\omega t} \sum_{n=-\infty}^{+\infty} i^n \mathcal{T}_n H_n^{(1)}(kr) e^{in\theta}. \tag{1}$$

Here $H_n^{(1)}$ is the Hankel function of the first kind and $\mathcal{T}_n = D_n^{(1)}/D_n$, where $D_n^{(1)}$ and D_n represent 6×6 determinants depending on the reduced frequency ka. They are determined from the boundary conditions. These are statements of continuity of stresses and displacements across the inner and the outer fluid-solid interfaces.[15] In Fig. 1, the real parts $\text{Re}(ka)$ of the roots of equation $D_n(ka) = 0$ are presented in the form of Regge trajectories (mode number versus resonance frequencies) for a steel shell surrounded by and filled with water. For each mode n there appear two
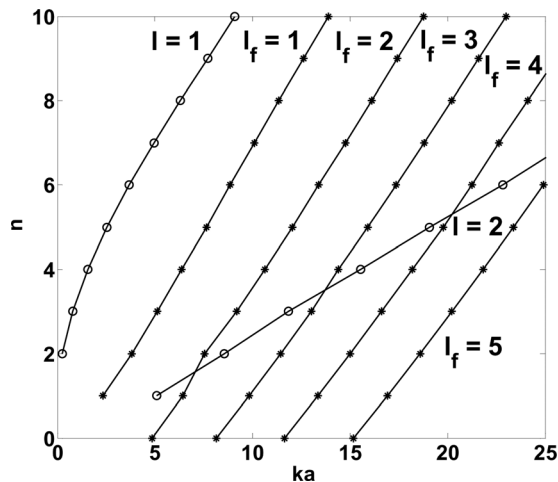
multiplicities $l = 1,2,\ldots$ and $l_f = 1,2,\ldots$ of resonances and the trajectories divide up into two sets labeled l and l_f, respectively. Computations and analysis show that the resonances (n,l_f) can be connected to the water column and the resonances (n,l) to the empty elastic shell. Each trajectory l or l_f is in relation with a circumferential wave around the shell. The numerical results are close to those given in Refs. 2 and 15. As it will be seen, these waves play an important role in the scattering by linear gratings as well as by two-dimensional gratings. The influence of the shell's thickness on the Regge trajectory for $l = 1$ is presented in Fig. 2. Significant shifts occur for high values of the modes n.

III. REFLECTION AND TRANSMISSION BY A LINEAR GRATING OF SHELLS

A. Theoretical background

The fluid medium considered above now contains an infinite number of circular cylindrical shells such as described in Sec. II, periodically spaced along the y direction with a spacing d; see Fig. 3. This linear periodic structure, referred to as the grating or the row can be considered as a reticular plane in free-field. When insonified by a plane harmonic pressure wave $p_{inc} = e^{-i\omega t} e^{i(k\cos\alpha x + k\sin\alpha y)}$, where α is the angle of incidence, it generates reflected, p_R, and transmitted, p_T, pressure waves of the form[1–3,12]

$$p_R = e^{-i\omega t} \sum_{\varepsilon=-\infty}^{+\infty} R_\varepsilon e^{i(-k_\varepsilon x + \ell_\varepsilon y)} \quad (x < 0), \tag{2}$$

$$p_T = e^{-i\omega t} \sum_{\varepsilon=-\infty}^{+\infty} T_\varepsilon e^{i(k_\varepsilon x + \ell_\varepsilon y)} \quad (x > 0), \tag{3}$$

representing a superposition of waves diffracted at different angles. Here, $k_\varepsilon = (k^2 - \ell_\varepsilon^2)^{1/2}$, $\ell_\varepsilon = k \sin\alpha + 2\pi\varepsilon/d$, and

$$R_\varepsilon = \frac{2}{k_\varepsilon d} \sum_{m=-\infty}^{m=+\infty} \mathcal{C}_m \mathcal{L}_{m\varepsilon}^+, \tag{4}$$

FIG. 1. First Regge trajectories of the circumferential waves for scattering by a water-filled steel shell with $b/a = 75/85$ in water.
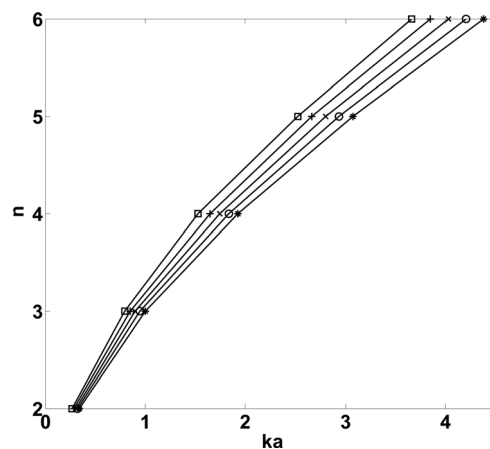

FIG. 2. Evolution of the Regge trajectory $l = 1$ for a water-filled steel shell at different b/a when the inner radius b varies by step of 0.5: $b/a = 75/85$ (□) to $73/85$ (∗).
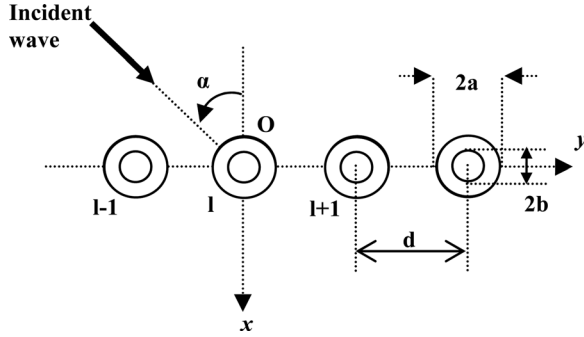
FIG. 3. Geometry for a linear grating of cylindrical shells.

$$T_\varepsilon = \delta_{0\varepsilon} + \frac{2}{k_\varepsilon d} \sum_{m=-\infty}^{m=+\infty} \mathcal{C}_m \mathcal{L}_{m\varepsilon}^- \tag{5}$$

are the reflection and transmission coefficients in the diffraction order ε, respectively, with $\mathcal{L}_{m\varepsilon}^\pm = (\ell_\varepsilon \pm i k_\varepsilon)^m / k^m$ and $\delta_{0\varepsilon} = 1$ if $\varepsilon = 0$ and $\delta_{0\varepsilon} = 0$, otherwise. In Eqs. (4) and (5), $\mathcal{C}_m$ represents the multiple scattering coefficient[1,12] of order m for the grating. For a fixed angle of incidence, α, the coefficients $\mathcal{C}_m$ are calculated by means of the following linear system:

$$\sum_{m=-\infty}^{m=+\infty} [\delta_{mn} - \mathcal{T}_n \sigma(m-n, \alpha)] \mathcal{C}_m = \mathcal{T}_n A_n, \tag{6}$$

where $\mathcal{T}_n$ is the scattering coefficient for one shell in free field and $A_n = i^n e^{-in\alpha}$. This infinite system is actually truncated to obtain a finite system, but the number of terms retained must be sufficient to ensure the stability of the solutions. The function σ denotes the Schlömilch series[16] defined as

$$\sigma(2q, \alpha) = 2(-1)^q \sum_{p=1}^{+\infty} H_{2q}^{(1)}(pkd) \cos(pdk \sin \alpha), \tag{7}$$

$$\sigma(2q+1, \alpha) = 2(-1)^q \sum_{p=1}^{+\infty} H_{2q+1}^{(1)}(pkd) \sin(pdk \sin \alpha), \tag{8}$$

where $q = 0, \pm 1, \pm 2, \ldots$. These series converge very slowly, so it is necessary for purposes of numerical calculations (duration and error reductions) to transform them into analytical expressions.[17]

When $d < \lambda$, where λ denotes the fluid wavelength, the grating is characterized by the zeroth order reflection and transmission coefficients R_0 and T_0, i.e., only one direction of propagation exists for the scattered waves ($\varepsilon = 0$). At normal incidence where $\alpha = 0$ (the incident pressure is exactly as defined in Sec. II), one obtains $\mathcal{L}_{m\varepsilon}^\pm = i^{\pm m}$ and

$$R_0 = \frac{2}{kd} \sum_{m=-\infty}^{+\infty} i^m \mathcal{C}_m, \tag{9}$$

$$T_0 = 1 + \frac{2}{kd} \sum_{m=-\infty}^{+\infty} i^{-m} \mathcal{C}_m. \tag{10}$$

B. Numerical results

Computations of the reflection coefficient R_0 for steel shells with $b/a = 75/85$ and $d/a = 2.65$ are presented in Figs. 4(a) and 4(b), respectively, for the reduced frequency range 0.1–7. The resonances (n,l) of individual shells presented in Sec. II can be identified easily on the curves. The resonances (n, l_f) occur for relatively higher frequencies, the first being located at $ka \simeq 2.33$ (near the first cutoff frequency $ka \simeq 2.37$ separating the domains $d < \lambda$ and $d > \lambda$). The resonances $(n,1)$ $(n = 2,3,4)$ of the Rayleigh wave have a nonnegligible influence[2] on the reflection and transmission properties of the row, especially in the frequency range 0.1–2.2. No significant shift is observed between resonance frequencies of one row and those of a single shell. An extension of computations for the reflection coefficient beyond the cutoff frequency is presented in Fig. 4(b). Note that from the results presented in Fig. 2, if a ratio $b/a = 73/85$ were considered in place of $b/a = 75/85$, the resonances observed in the reflection coefficient would be shifted from the low frequencies to higher ones within the frequency range 0.1–2.2, the largest shifts occurring for the resonances (3,1) and (4,1).

IV. ENGINEERING PASS BANDS AND STOP BANDS

In this section, we analyze the properties of several kinds of two-dimensional gratings. Three of these structures
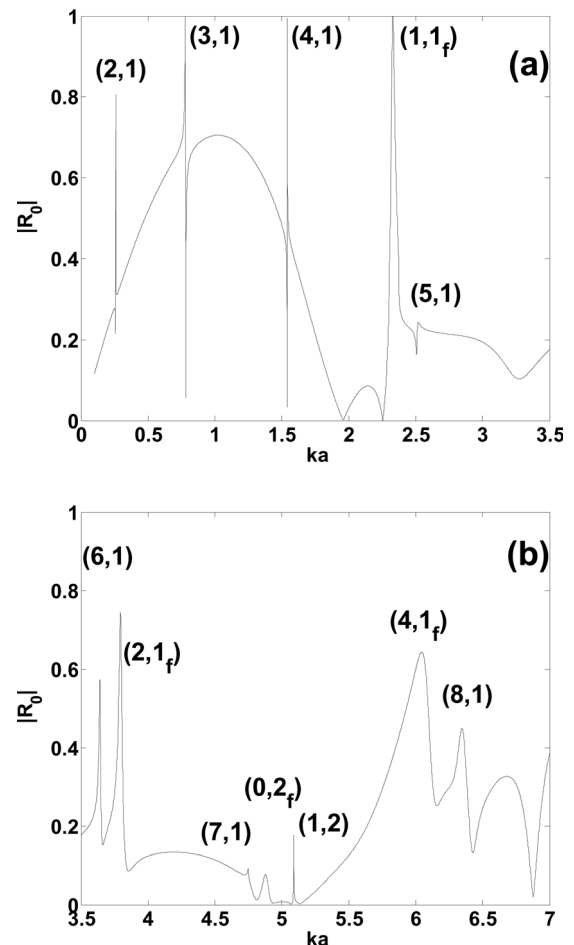

FIG. 4. Modulus of the reflection coefficient for a linear grating of steel shells with $b/a = 75/85$ and $d/a = 2.65$ for the diffraction order $\varepsilon = 0$.

Zong et al.: Perturbations in phononic crystals

are presented in Figs. 5(a)–5(c). They are often referred to as phononic crystals, or as two-dimensional lattices. We consider N parallel rows of infinite extent along the Oy direction perpendicular to the direction of the incident waves materialized by the thick arrows in Figs. 5(a)–5(c). To obtain the reflection and transmission coefficients at normal incidence by N rows, one must first calculate the reflection and transmission coefficients R_j and T_j by the individual rows ($1 < j < N$), bearing in mind that the physical parameters can differ from row to row. One can build the reflection and transmission coefficients of a sequence of j rows, $R(j)$ and $T(j)$, by using a recurrence relationship involving the reflection and transmission coefficients of $(j-1)$ rows together with the coefficients R_j and T_j. We use either $R(j-1)$ and $T(j-1)$ if the incident wave propagates in the direction of increasing values of x or R_{dj}, $R_d(j-1)$ and $T_d(j-1)$ $\equiv T(j-1)$ when the incident wave propagates in the opposite direction [see Eqs (11)–(13)]. Between the set of $(j-1)$ rows and the jth row separated by the distance D_{j-1}, there exist multiple reflections and transmissions. By superimposing all the contributions for the reflection on the one hand and the transmission on the other, and next by using a recurrence method, it can be shown that

$$R(j) = R(j-1) + \frac{R_j T^2(j-1)e^{i\varphi_{(j-1)R}}}{1 - R_d(j-1)R_j e^{i\varphi_{(j-1)R}}}, \tag{11}$$

$$T(j) = \frac{T(j-1)T_j e^{i\varphi_{(j-1)T}}}{1 - R_d(j-1)R_j e^{2i\varphi_{(j-1)T}}}, \tag{12}$$

$$R_d(j) = R_{dj} + \frac{T_j^2 R_d(j-1)e^{i\varphi_{(j-1)R}}}{1 - R_d(j-1)R_j e^{i\varphi_{(j-1)R}}}, \tag{13}$$

where $\varphi_{(j-1)R} = 2\varphi_{(j-1)T}$ with $\varphi_{(j-1)T} = kD_{j-1}$ (case of normal incidence). This is the essence of the Debye series method very similar to the Fabry-Pérot method used in optics. These relationships remain valid in the case where all the rows are identical, the coefficients being $R_j = R_{dj} \equiv R_0$, $T_j \equiv T_0$, $\forall j > 1$ or in the case where the period is a multilayer (a set of several rows) with coefficients for the zeroth diffraction order $\tilde{R}_0$, $\tilde{R}_{0d}$, and $\tilde{T}_0$. This implies $R_j \equiv \tilde{R}_0$, $R_{dj} \equiv \tilde{R}_{0d}$, $T_j \equiv \tilde{T}_0$. Such

a method is a version of that described in Ref. 3, and further details concerning a generalization can be found in Ref. 11.

A. Stop bands of periodic phononic crystals

We consider first the phononic crystal described in Fig. 5(a) made up of ten identical rows containing shells with $b/a = 75/85$. A regular spacing $D/a = 3$ between rows is accounted for. Figure 6(a) presents the transmission coefficient versus the reduced frequency ka for a spacing between shells in a row $d/a = 2.65$. A stop band corresponding to a frequency domain of null transmission can be observed in the range of ka 0.8–1.3. Figure 6(b) obtained with a spacing between shells $d/a = 2.3$ shows that the stop band is widened. We observe undulations on both sides of the stop bands. We also observe the steel row resonances (2,1), (3,1), and (4,1). Except for the appearance of the resonances, similar results are shown in Fig. 11 of Ref. 18.

For an infinite number of any kind of period with reflection coefficients $\tilde{R}_0$ at one face and $\tilde{R}_{0d}$ at the opposite face (the transmission coefficient $\tilde{T}_0$ is the same whatever face is insonified), the dispersion equation is required for the study of the wave propagating through the infinite structure. By applying the periodic conditions for the pressure and for the displacement fields in points located exactly one period apart, it can be shown that the dispersion equation for the Bloch wavenumber k_{eq} versus ka is given by
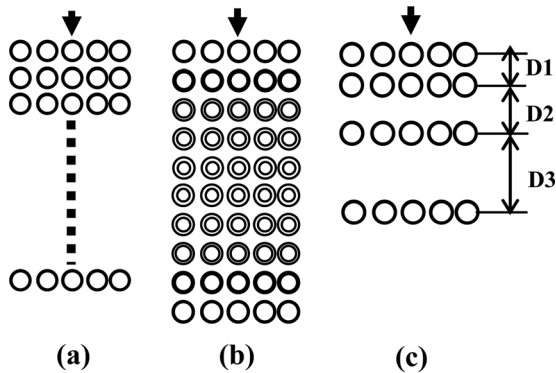

FIG. 5. Geometry for the two-dimensional phononic crystals. (a) Rectangular lattice, (b) lattice with inner radius of shell b varying from row to row: $73/85 \le b/a \le 75/85$, (c) lattice with irregular spacing D/a between rows.
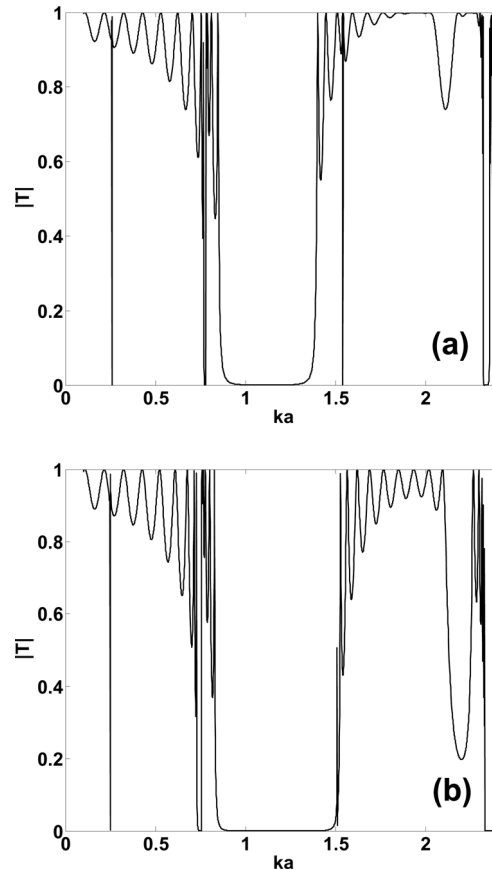
FIG. 6. Modulus of the transmission coefficient for a two-dimensional phononic crystal made up of ten identical rows with $b/a = 75/85$ and $D/a = 3$. (a) $d/a = 2.65$, (b) $d/a = 2.3$.

$$\cos(k_{eq}D) = \frac{1}{2\tilde{T}_0}[\cos kD(\tilde{T}_0^2 - \tilde{R}_0\tilde{R}_{0d} + 1)$$
$$+ i\sin kD(\tilde{T}_0^2 - \tilde{R}_0\tilde{R}_{0d} - 1)]. \qquad (14)$$

In the case where the period contains only one row for instance, we have $\tilde{R}_0 = \tilde{R}_{0d}$ and Eq. (14) becomes Eq. (39) of Ref. 2. We present in Fig. 7 dispersion curves, i.e., the real part of the normalized Bloch wavenumber $k_{eq}D/\pi$ versus ka. We consider two rectangular lattices with $D/a = 3$, the one with $d/a = 2.65$ (solid curve), the other with $d/a = 2.3$ (dotted curve). In each case, there exist two band gaps: the first gap is a confirmation of results observable in Fig. 6(b), the second is a consequence of the dip in the transmission coefficient in the reduced frequency range 2–2.25. Computations of the transmission coefficients not presented here showed us that the depth of the dip increases with the number of rows and that the stop bands do not change when the inner radius of the shell is modified. Further, each dispersion curve in Fig. 7 exhibits resonances at the same locations as the ones for single rows in Fig. 4.

B. Engineering multiple narrow pass bands in large stop bands with irregular shell thicknesses

Some treatments can be carried out[4] to create selective frequency filters in the stop band of phononic crystals by using square lattices. In this paper, we consider graded rectangular lattices as sketched in Fig. 5(b) with $D/a = 3$, $d/a = 2.65$, and b/a successively equal to 75/85 (insonified face, first row), 74.5/85, 74/85, 73.5/85, and 73/85 (symmetry line of the crystal). Thus, the outer radius of the shells remains constant while the inner radius varies from row to row. The transmission coefficient of this graded phononic crystal is presented in Fig. 8. It exhibits four narrow pass bands in the frequency domain 0.9–1 included in the large stop band presented in Fig. 6(a). The fifth narrow pass band is located at the left border of the stop band. It corresponds to the resonance (3,1) of the rows with shells of b/a ranging from 73/75 to 75/85. The five minimums in the frequency ranges 0.25–0.35 and 1.55–1.8 are related to the resonances

FIG. 8. Modulus of the transmission coefficient for the lattice sketched in Fig. 5(b) with $d/a = 2.65$ and $D/a = 3$.

(2,1) and (4,1), respectively, for the different values of b/a. These observations are in agreement with the evolutions of the Regge trajectories shown in Fig. 2. So, when the lattice contains rows with five different values of shell thickness,

FIG. 9. Transmission coefficients for two-dimensional phononic crystals made up of shells with $b/a = 75/85$ and $d/a = 2.65$ showing the evolution of the stop band. (a) 100 rows regularly spaced of $D/a = 3$, (b) 100 rows spaced according to the rule $D/a = N \times 0.1 + 3$ ($0 \le N \le 99$).
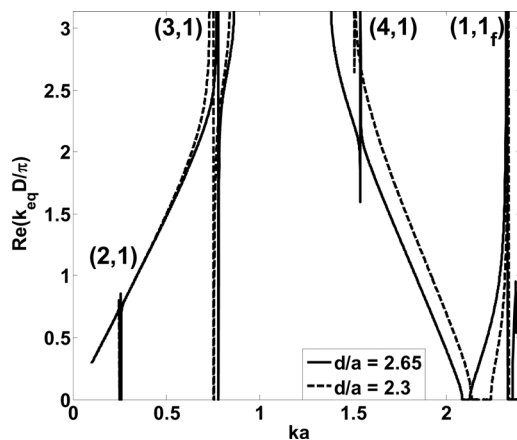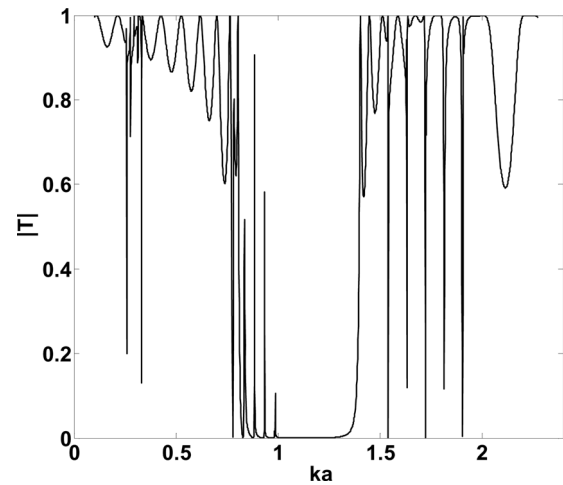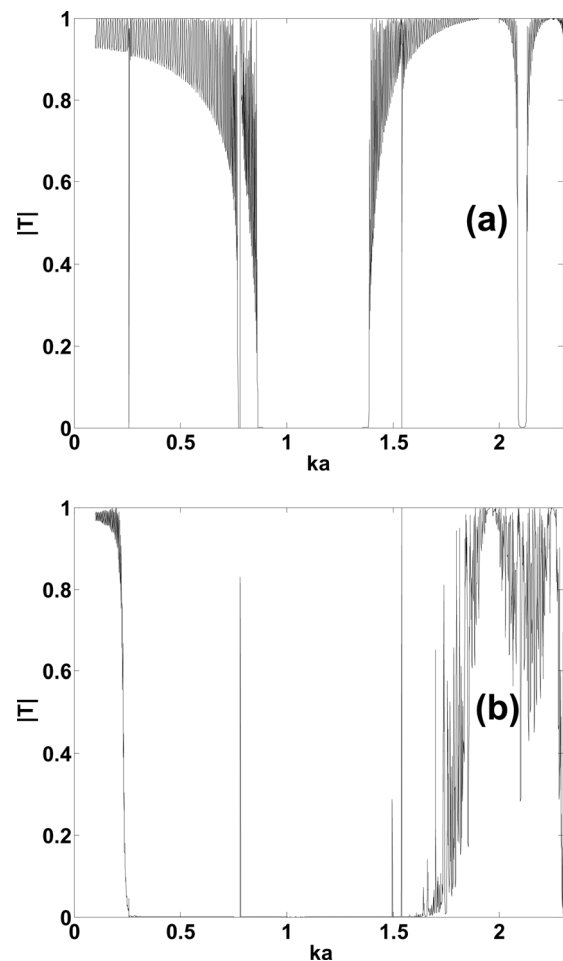

FIG. 7. Dispersion curves for infinite two-dimensional phononic crystals. Case of steel shells with $b/a = 75/85$ and $D/a = 3$. Solid curve: $d/a = 2.65$, dotted curve: $d/a = 2.3$.

Zong *et al.*: Perturbations in phononic crystals

there is a degeneracy at order five of the resonances. It can be generalized to any value of b/a. Khelif *et al.*[4] reported that the transmission coefficient of a mixed structure composed of a square lattice of shells with different inner radii (same outer radii) arranged in successive rows may be constructed from the transmitted signal of one of the rows with several narrow pass bands inside the stop band. It can be noted also that the lattice with b/a varying from 73/85 (insonified face, first row) to 75/85 (symmetry line of the crystal) leads to the same conclusions.

C. Widening of stop band using increasing spacing between rows

Transmission coefficients by lattices with different patterns of increasing spacings between 20 rows were first studied in Ref. 12. They showed that a fixed spacing strategy rather than a variable spacing strategy improves transmission in the incident direction over the full range of frequencies. This gave us the idea that the strongest modification of the transmission can occur for a greater number of rows. To this end, calculations of the transmission coefficients are performed for lattices with increasing spacings D/a between rows sketched in Fig. 5(c). Our example accounts for shells

with $b/a = 75/85$, $d/a = 2.65$, and the rule $D/a = N \times 0.1 + 3$, with $N = 0$ between the two first rows. Quantitatively, this means that with shells of outer radius $a = 0.2$ cm the lattice is 6.1 cm long with 10 rows and 1.6 m long for 100 rows. The results are presented for ka ranging from 0.1 to 2.37; this is equivalent to the frequency domain 11.7–277.2 kHz. In Fig. 9(a), the transmission coefficient for 100 rows regularly spaced ($D/a = 3$) shows a stop band similar to that found for 10 rows in Fig. 6(a). Further, by increasing the spacing between the rows the stop band of reference given in Fig. 9(a) widens on its two sides, Fig. 9(b). At low frequency the stop band is approximately bounded by the shell resonance (2,1) ($ka = 0.27$) and at high frequency by the resonance (4,1) ($ka = 1.56$). For a higher number of rows, the right limit of the stop band shifts toward higher frequencies. Narrow pass bands are located at $ka \simeq 0.8$ [shell resonance (3,1)] and at $ka = 1.56$. The peak located at $ka \simeq 1.50$ is not a resonance and vanishes as the number of rows increases. So, in the stop band, the only way for transmitting acoustic waves is to select the frequencies of the resonances (2,1), (3,1), and (4,1) of the single shell. We have thus demonstrated that a large band gap can be created from the stop band of reference of a regular lattice by considering an irregular spacing between rows of shells.
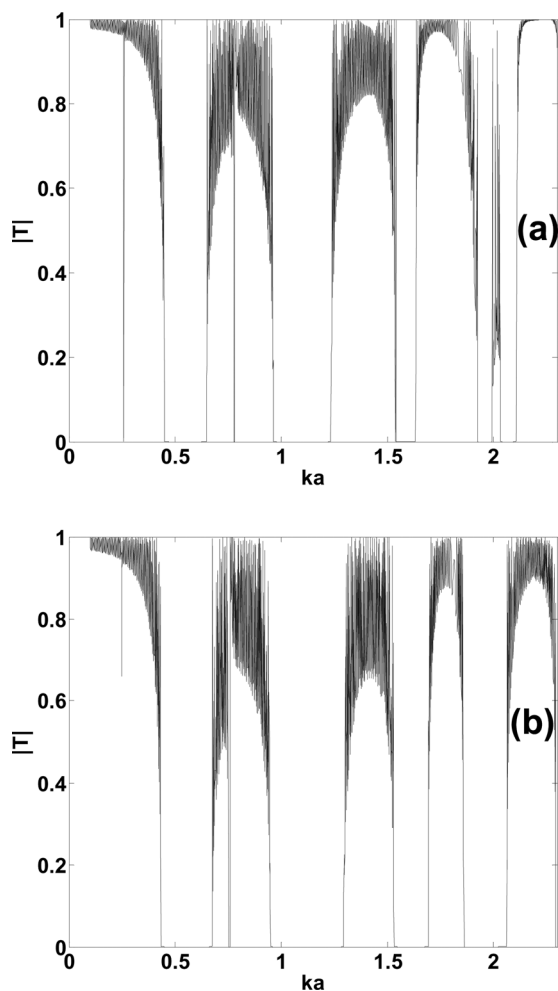

FIG. 10. Transmission coefficients for a two-dimensional phononic crystal made of 100 bilayers of one steel row and one polyethylene row of same d/a: (a) $d/a = 2.65$, (b) $d/a = 2.3$; shells with $b/a = 75/85$ and $D/a = 3$.
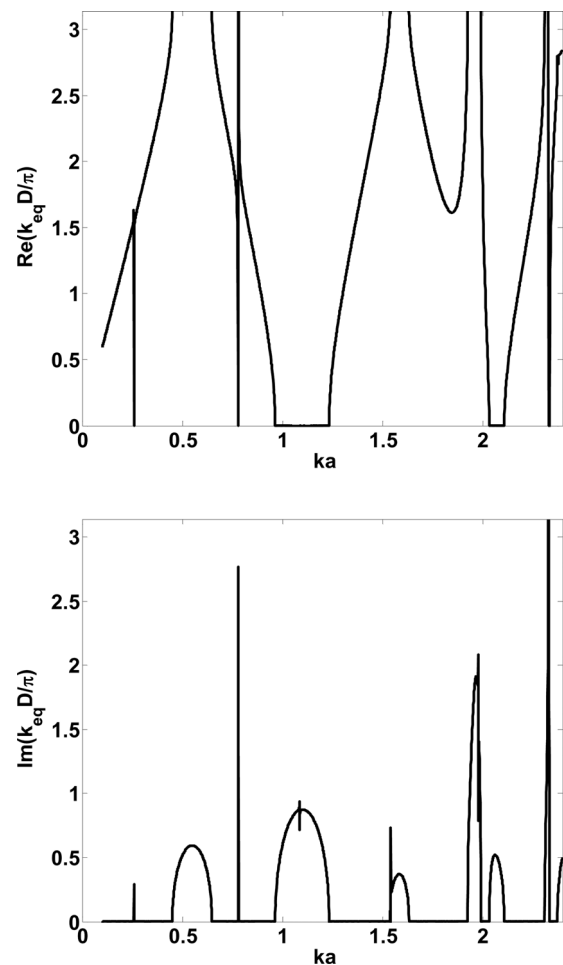

FIG. 11. Dispersion curves for infinite two-dimensional phononic crystals using bilayers. $b/a = 75/85$, $d/a = 2.65$, and $D/a = 3$. (a) Real part and (b) imaginary part of the normalized Bloch wavenumber $k_{eq}D/\pi$ versus ka.

D. Widening of stop band using increasing spacing between rows of bilayer materials

By bilayers, we mean a structure made of two parallel rows of shells of different materials. The analysis is carried out by considering steel shells in the first row and polyethylene shells in the second row. The physical parameters of the latter material are $\rho_p = 940 \, \text{kg/m}^3$ (density), and $c_l = 2370$ m/s and $c_t = 800$ m/s (longitudinal and transverse velocities, respectively). All the shells have a thickness ratio $b/a = 75/85$. Two values of the spacing d/a between shells in a given row are chosen for our computations.

At first, the transmission coefficients for a phononic crystal made of 100 bilayers containing a steel row and a polyethylene one with the same spacing between rows ($D/a = 3$) are presented. In Fig. 10(a) it is plotted for the same $d/a = 2.65$ and in Fig. 10(b) for the same $d/a = 2.3$ in each row. In Fig. 10(a), we observe five stop bands, and the steel row resonances (2,1) and (3,1) are located in the first two wide pass bands. No resonances of the polyethylene row are detected in the studied frequency range. *A priori*, according to the study of a single polyethylene row, resonances (1,1) and (2,1) could be observed. However, the half-widths of those resonances are very small compared to the half-widths of the steel row resonances, so they do not appear in

the transmission coefficient by one or several bilayers. We can observe similar results in Fig. 10(b). However, only four stop bands are detected. We also note a widening of the stop bands with regard to the first four in Fig. 10(a). The dispersion curve for an infinite lattice of bilayers can be obtained from Eq. (14). In Figs. 11(a) and 11(b) the real part and the imaginary part of the normalized Bloch wavenumber $k_{eq}D/\pi$ are plotted versus ka for bilayers with $d/a = 2.65$. Five stop bands are observed in the ka intervals 0.45–0.65, 0.96–1.23, 1.54–1.63, 1.92–1.99, and 2.03–2.10, on the plots of the real and the imaginary parts. They correspond to the stop bands exhibited in the plot of the transmission coefficient in Fig. 10(a). The steel row resonances (2,1) at $ka = 0.27$, (3,1) at $ka = 0.8$, and (4,1) at $ka = 1.56$ are detected. It is also the case for the polyethylene row resonances (1,1) at $ka = 1.08$ and (2,1) at $ka = 2.08$, which are not present in the transmission coefficient in Fig. 10(a).

Now we study the transmission coefficients of 100 bilayers differently spaced according to the rule $D/a = N \times 0.1 + 3$ ($0 \leq N \leq 99$). Transmission coefficients are plotted in Fig. 12(a) for the same $d/a = 2.65$ and in Fig. 12(b) for the same $d/a = 2.3$. In each figure, very large stop
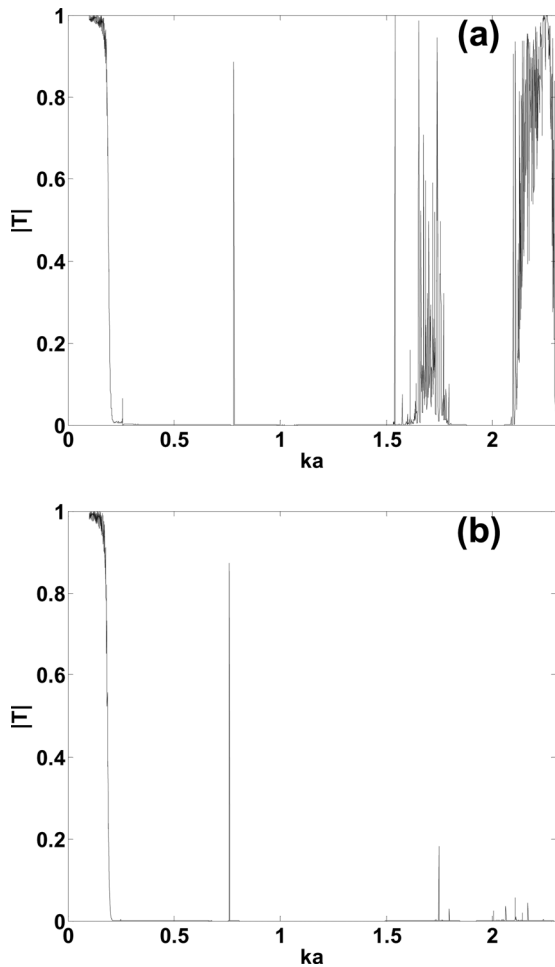

FIG. 12. Transmission coefficients for a two-dimensional phononic crystal of 100 bilayers spaced according to the rule $D/a = N \times 0.1 + 3$ ($0 \leq N \leq 99$): (a) $d/a = 2.65$, (b) $d/a = 2.3$; shells with $b/a = 75/85$.
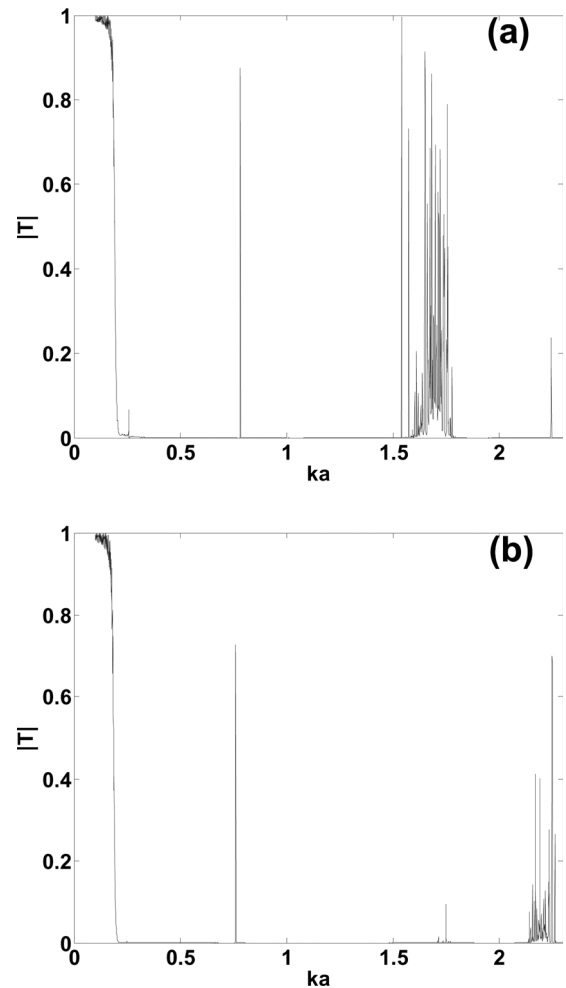

FIG. 13. Transmission coefficients for a two-dimensional phononic crystal made of 100 bilayers spaced according to the rule $D/a = N \times 0.1 + 3$ ($0 \leq N \leq 99$): (a) one steel row with $d/a = 2.65$ and one polyethylene row with $d/a = 2.3$, (b) one steel row with $d/a = 2.3$ and one polyethylene row with $d/a = 2.65$; shells with $b/a = 75/85$.

bands are observed in frequency intervals ranging from 0.2 to values greater than 2 as well as a thin pass band linked with the resonance (2,1) of a steel row. We also note that the pass bands between 1.5 and 2.3 in Fig. 12(a) disappear in Fig. 12(b).

We can also break the symmetry in the bilayer by choosing different spacings d/a in each row. In this context, transmission coefficients are plotted in Fig. 13(a) for $d/a = 2.65$ in the steel row and $d/a = 2.3$ in the polyethylene row, and in Fig. 13(b) for $d/a = 2.3$ in the steel row and $d/a = 2.65$ in the polyethylene row. Nearly the same observations as in Figs. 12(a) and 12(b) can be made, namely, the widening of stop bands compared to those of Figs. 10(a) and 10(b). However, as shown by comparing Figs. 12(a) and 13(a), quite large pass bands are no longer detected at high frequency. The study of this type of media at oblique incidence ($\alpha = 0°$ to $\alpha = 45°$) shows similar results.

V. CONCLUSION

The combination of a multiple scattering technique between shells and of a Debye series method between rows provides a numerically efficient tool for the study of reflection, transmission, and band gap engineering of phononic crystals. This tool remains stable under perturbations of the periodicity of phononic crystals. We perform computations for structures containing up to 100 rows. The first example concerns a structure in which the inner radius of shells is varied from row to row. As a result, it is shown that several acoustic narrow pass bands created in the existing stop bands permit transmission at multiple selective frequencies. The second example deals with structure arranged in such a way that the spacing from row to row increases or decreases from the insonified row. It is observed that the stop bands of reference of regular lattices are enlarged when we consider irregular spacings between rows. In the third example, we consider structures made up of steel-polyethylene bilayers instead of single steel rows. For the same spacing rule between rows, the high contrast existing between the two materials ensures a widening of the stop bands with regard to the case where only steel rows were used. In the last example, it has also been observed that the difference in spacing between the shells forming a bilayer can modify the stop band.

The aim of this theoretical study is to verify the feasibility of underwater silent materials or acoustic filters. Our work involves monolayer shells in order to obtain very large stop bands. Other practical solutions exist. For instance, steel shells coated with silicone rubber can be used to create strongly attenuating devices, as presented in Ref. 19.

The study presented in this paper deals with the frequency domain, and the case of higher diffraction orders occurring beyond the first cutoff frequencies relative to each row is not investigated. Further simulations in the time domain have been carried out and make it possible to predict that these kinds of phononic crystals may be used for acoustic beam focalization or deviation. These results are out of the scope of this paper and will be presented later.

[1] C. Audoly and G. Dumery, "Modeling of compliant tube underwater reflectors," J. Acoust. Soc. Am. **87**(5), 1841–1846 (1990).

[2] M. A. Heckl, "Sound propagation in bundles of periodically arranged cylindrical tubes," Acustica **77**, 143–152 (1992).

[3] X. Y. Huang and M. A. Heckl, "Transmission and dissipation of sound waves in tube bundles," Acustica **78**, 191–200 (1993).

[4] A. Khelif, P. A. Deymier, B. Djafari-Rouhani, J. O. Vasseur, and L. Dobrzynski, "Two-dimensional phononic crystal with tunable narrow pass-band: Application to a waveguide with selective frequency," J. Appl. Phys. **94**(3), 1308–1311 (2003).

[5] L. Sanchis, F. Cervera, J. Sanchez-Dehesa, J. V. Sanchez-Perez, C. Rubio, and R. Martinez-Sala, "Reflectance properties of two-dimensional sonic band-gaps crystals," J. Acoust. Soc. Am. **109**(6), 2598–2605 (2001).

[6] Y. Lai, X. Zhang, and Z.-Q. Zhang, "Engineering acoustic band gaps," Appl. Phys. Lett. **79**(20), 3224–3226 (2001).

[7] Y. Lai and Z.-Q. Zhang, "Large band gaps in elastic phononic crystals with air inclusions," Appl. Phys. Lett. **83**(19), 3900–3902 (2003).

[8] V. Twersky, "On scattering of waves by the infinite grating of circular cylinders," IEEE Trans. Antennas Propag. **10**, 737–765 (1962).

[9] P. A. Martin, *Multiple Scattering: Interaction of Time-Harmonic Waves with N Obstacles* (Cambridge University Press, Cambridge, 2006), pp. 1–450.

[10] C. Qiu, Z. Liu, J. Mei, and M. Ke, "The layer multiple-scattering method for calculating transmission coefficients of 2D phononic crystals," Solid State Commun. **134**, 765–770 (2005).

[11] R. Sainidou, N. Stefanou, I. E. Pasrobas, and A. Modinos, "A layer-multiple scattering method for phononic crystals and heterostructures of such," Comput. Phys. Commun. **166**, 197–240 (2005).

[12] L. S. Mulholland and M. A. Heckl, "Multi-directional sound wave propagation through a tube bundle," J. Sound Vib. **176**(3), 377–398 (1994).

[13] S. Robert, J.-M. Conoir, H. Franklin, and F. Luppé, "Resonant elastic scattering by a finite number of cylindrical cavities in an elastic matrix," Wave Motion **40**, 225–239 (2004).

[14] L. Flax, G. C. Gaunaurd, and H. Überall, "Theory of resonance scattering," in *Physical Acoustics. Principles and Methods*, Vol. 15, edited by W. P. Mason and R. N. Thurston (Academic, New York, 1981), pp. 191–293.

[15] N. D. Veksler, "Sound wave scattering by circular cylindrical shells," Wave Motion **8**, 525–536 (1986).

[16] V. Twersky, "Elementary representations of Schlömilch series," Arch. Ration. Mech. Anal. **8**, 323–332 (1961).

[17] C. M. Linton, "Schlömilch series that arise in diffraction theory and their efficient computation," J. Phys. A: Math. Gen. **39**, 3325–3339 (2006).

[18] P. McIver, "Water-wave propagation through an infinite array of cylindrical structures," J. Fluid Mech. **424**, 101–125 (2000).

[19] M. Hirsekorn, P. P. Delsanto, N. K. Batra, and P. Matic, "Modelling and simulation of acoustic wave propagation in locally resonant sonic materials," Ultrasonics **42**, 231–235 (2004).